Diabetes, Metabolic Syndrome and Obesity

Dovepress
Taylor & Francis Group

Open Access Full Text Article

ORIGINAL RESEARCH

Metformin Activation of Sirtuin 3 Signaling Regulates Mitochondrial Function Improves Diabetes-Associated Cognitive Impairment

Jiang-Fei An[1–3,*], Hang Su[1–3,*], Chun-Qiang Zhang[1–3], Xue-Ting Wang[1–3], Guang-Qiong Zhang[1–3], Ling-Yun Fu[1–3], Yi-Ni Xu[1–3], Ling Tao[1–3], Xiang-Chun Shen[1–3]

[1]The State Key Laboratory of Functions and Applications of Medicinal Plants, Guizhou Medical University, Guiyang, Guizhou, 561113, People's Republic of China; [2]The High Efficacy Application of Natural Medicinal Resources Engineering Center of Guizhou Province, School of Pharmaceutical Sciences, Guizhou Medical University, Guiyang, Guizhou, 561113, People's Republic of China; [3]The Key Laboratory of Optimal Utilization of Natural Medicine Resources, School of Pharmaceutical Sciences, Guizhou Medical University, Guiyang, Guizhou, 561113, People's Republic of China

*These authors contributed equally to this work

Correspondence: Xiang-Chun Shen, Email shenxiangchun@126.com

Context: Diabetes-associated cognitive impairment (DACD) is a prevalent complication of diabetes mellitus, with a strong correlation to both the severity and duration of the disease. While metformin has demonstrated a significant impact on mitigating DACD, the precise mechanisms underlying its therapeutic effects remain inadequately understood.

Objective: This study aims to examine the protective effects of metformin (MET) on DACD and to elucidate the underlying mechanisms involved.

Materials and Methods: C57BL/6J male mice from in vivo animal experiments established DACD by high-fat diet (HFD) for 12 weeks, combined with intraperitoneal injection of low-dose streptozotocin (STZ, 40 mg/kg). Subsequently, DACD mice were administered MET for 2 months. The expression levels of proteins related to mitochondrial function were analyzed using immunohistochemical staining, immunofluorescence double staining, qRT-PCR, and Western blot. Furthermore, the mechanism underlying the improvement of DACD by MET was validated by using the Sirtuin 3 (SIRT3) agonist resveratrol (RES), the inhibitor 3-TYP, and sh-SIRT3 on astrocytes.

Results: Our findings indicate that MET significantly ameliorated mitochondrial dysfunction in DACD mice, accompanied by an upregulation of SIRT3 expression. Furthermore, comparable results were noted with the SIRT3 agonist RES. Meanwhile, suppressing SIRT3 expression via sh-SIRT3 or SIRT3 inhibitor 3-TYP in astrocytes largely abolished MET's ability to restore mitochondrial function.

Conclusion: It has been demonstrated that MET ameliorates mitochondrial dysfunction by activating the SIRT3 signaling pathway to rescue DACD.

Keywords: metformin, sirtuin 3, mitochondria, diabetes-associated cognitive dysfunction, astrocytes

Introduction

Diabetes mellitus (DM) is defined as a chronic metabolic disorder and constitutes one of the most rapidly expanding chronic diseases globally. Furthermore, according to pertinent statistics, the global DM patients have exceeded 463 million in 2019, with projections indicating that this number will escalate to 702 million by 2045.[1] Consequently, the incidence of diabetes-associated cognitive dysfunction (DACD) is 13.5%, significantly higher than that in non-diabetic individuals.[2] DACD typically pertains to diabetic patients with varying degrees of cognitive impairment, mental abnormalities and dementia.[3] Notably, DACD in elderly individuals may represent an early stage in the onset of dementia. Dementia, characterized by acquired cognitive dysfunction as its primary core, leads to a significant decline in patients' study, work, and daily life.[4] Currently, DACD has emerged as a widespread chronic disease globally.

Received: 10 January 2025
Accepted: 23 June 2025
Published: 12 July 2025

Consequently, it is of great significance to deeply study the pathogenesis of patients and to find better treatment means and appropriate targets of patients.

Astrocytes (AST) in the DACD patients brain play a crucial role, specifically, primary astroglial fine, which are the most abundant and widely distributed glial cells in the central nervous system,[5] are instrumental in regulating the formation and maintenance of the blood-brain barrier. Furthermore, these cells influence the formation of synapses, as well as the development and plasticity of neurons.[6] AST is a vital bridge connecting neurons and blood vessels.[7] Notably, AST possesses a highly prominent glycolytic capacity, enabling it to generate energy through glycolysis. This characteristic allows astrocytes to combat damage resulting from mitochondrial dysfunction and to exhibit a stronger antioxidant capacity compared to neurons.[8] Consequently, AST plays a pivotal role in maintaining the health and function of the central nervous system. Given that astrocytes possess the ability to transfer mitochondria, they play a crucial role in promoting neuronal survival.[9] A healthy mitochondrial state may therefore be indispensable for astrocytes to produce neuroprotective mechanisms, essential for maintaining the energy balance of the brain and safeguarding the production of antioxidants in neurons.[10,11] Research has shown that the development of DACD is accompanied by disorders in mitochondrial fusion and fission.[12] Mitochondria is a highly dynamic organelle, and the dynamic changing balance of mitochondrial fission and fusion has important implications for DACD development.[13]

Sirtuin 3 (SIRT3) is predominantly distributed in the mitochondrial matrix and possesses robust deacetylation capabilities. As such, SIRT3 plays a pivotal role in maintaining mitochondrial homeostasis.[14] SIRT3 exhibits an ameliorative effect on DACD by inhibiting the membrane abnormalities associated with mitochondria and mitigating the mitochondrial dysfunction induced by mitochondrial Ca^{+} overload.[15] Complex V (ATP synthase), a key player in mitochondrial oxidative phosphorylation (OXPHOS), is essential for maintaining mitochondrial bioenergy and regulating oxidative free radicals,[16] such as participating in the generation of mitochondrial ATP and balancing mitochondrial membrane potential.[17] ATP5O protein (ATP synthase subunit O), an integral component of ATP synthase in mitochondria, is closely related to ATP generation.[18] Studies have shown that SIRT3 can enhance the deacetylation level of ATP5O in human clear cell renal cell carcinoma, thereby exerting the disease amelioration of the drug.[19] Currently, it remains unclear whether SIRT3's ability to deacetylate ATP5O can ameliorate DACD.

Metformin (MET), a prescription drug commonly utilized to treat type 2 diabetes (T2D), effectively reduces blood glucose levels while posing a minimal risk of hypoglycemia.[20] Related studies have demonstrated that MET's glucose-lowering effect is mainly mediated through selective inhibition of hepatic gluconeogenesis, with the contribution of microorganisms playing a secondary role.[21] However, the study of MET lowering blood glucose to improve diabetes is relatively perfect, but the investigation on DACD has not been extensively studied. Therefore, in this study, we aimed to address this gap by establishing a DACD model to explore how MET affects mitochondrial function mediated by SIRT3.

Materials and Methods

Animals

C57BL/6J male mice (18–22 g) were obtained from SPF (Beijing) biotechnology Co. Ltd, with an Animal Production License No.: SCXK (Jing) 2019–0010. Animal experiments conducted in this study adhered strictly to the guidelines established by the National Institutes of Health for the care and use of laboratory animals. These experiments were also approved by the Animal Ethics Committee of Guizhou Medical University (2402902), ensuring compliance with both the National Institutes of Health guidelines and the principles outlined in the Declaration of Helsinki. Following one week of adaptive feeding, the mice were divided into two groups: a normal feeding group and a high-fat feeding combined with STZ administration to induce the DACD model group. Subsequently, diabetic mice (fasting blood glucose levels ≥11.1 mmol/L) were divided into the DACD group and the MET treatment group. To ensure the accuracy of animal behavioral tests, we excluded mice with diabetic foot disease and diabetic retinopathy. Ultimately, each experimental group contained 16 mice. Upon completion of the MET drug treatment regimen, all mice were euthanized under isoflurane anesthesia for subsequent experimental procedures. The sample size calculation was performed according to the formula (Resource Equation Approach).

Morris Water Maze (MWM)

Morris water maze (MWM) experiments were conducted to assess spatial learning and memory abilities in DACD mice. Specifically, both the normal group of mice and those that had completed the drug treatment phase are subjected to the MWM experiments. The experimental scheme can be divided into training and learning part and test part.[22] Subsequently, the differences in learning and memory ability of each group were analyzed to compare the movement trajectory of each group.

Sucrose Preference Test (SPT)

The early phases of DACD were frequently accompanied by depressive-like behaviors. To investigate this, SPT was conducted on each group. The SPT values were calculated by comparing the sugar water intake and pure water intake in each group.

Forced Swim Test (FST)

Mice were placed into the prepared transparent cylinder for 6 min, and the duration of immobility after 5 min was recorded. Following testing for each mouse, the water in the cylinder was replaced to ensure consistency, maintaining the same depth throughout all trials.

Histological Dyeing

Mouse brain tissue was fixed using 4% paraformaldehyde and subsequently stained with hematoxylin-eosin and Masson trichrome dyes. The stained sections were then examined under a light microscope (Nikon Eclipse E100, Tokyo, Japan) for further analysis.

Transmission Electron Microscopic Analysis

Initially, the samples were fully removed. The staining process began with immersion in 3% glutaraldehyde, followed by treatment with 1% osmium tetroxide. Subsequent steps included dehydration and embedding. For optical localization, semi-thin sections were stained with methylene blue. For examination under the JEM-1400-FLASH transmission electron microscope, the sections were stained with uranyl acetate and lead citrate.

Separation and Purification of Primary Mouse Astrocytes

Newborn mice, aged 1–3 days, were soaked in 75% alcohol for one minute and then swiftly moved outside the ultra-clean table The cerebral cortex and blood vessels were dissected and surgically removed. After thoroughly washing away any bloodstains using PBS, the samples were transferred into a vial containing an appropriate amount of pre-cooled PBS. Then, the tissue was washed three times with an appropriate amount of PBS. Following this, the tissue was infiltrated with the appropriate double antibody. After another three washes with PBS (ensuring that the last wash was as dry as possible), the tissue was added to a vial containing a mixture of PBS and pancreatic enzyme =1:1. The mixture was thoroughly mixed, and the tissue was grouped and sealed with a sealing strip. The vial was then stored at 4°C overnight. After 12 hours, mix evenly in a 15 mL centrifuge (inhale PBS and pancreatic sin into the centrifuge tube 2:1), mix well with the dropper, and then digest in a 37°C 5% CO_2 incubator for 15 minutes. Following digestion, the process was terminated by adding 1 mL of 10% DMEM/HG medium. The mixture was thoroughly filtered using a pipette, centrifuged at 1000 rpm for 5 minutes, resuspended, and inoculated into a 25 cm^2 culture flask. In the evening, the fluid was changed, and then every two days (the culture bottle was treated by the cross method for 5 min to remove the weak microglial cells), until the cells were covered with 95% of the bottle and passaged.

After aspirating the old medium, 1 mL of 0.25% trypsin was added and the cells were observed under an inverted microscope. Once approximately 70% of the cells began to retract and form a circular shape, indicating that they were adequately detached, 2 mL of complete medium was promptly added to terminate the digestion process. Subsequently, the cell suspension was transferred to a 15 mL centrifuge tube and centrifuged at 1000 rpm for 5 minutes. Following centrifugation, the supernatant was discarded, and the cells were resuspended in complete medium. Finally, the

resuspended cells were inoculated into a new culture bottle. Continue in the incubator to 4–5 passages for subsequent experiments.

Immunohistochemical Staining

Immunohistochemistry (IHC) staining of the sections was successively dewaxed and hydrated. This was followed by antigen retrieval using sodium citrate buffer. After that, the sections were individually incubated with the primary antibodies anti-DRP1, anti-FIS1, anti-MFN1, anti-MFN2, anti-SIRT3 and anti-ATP5O (1:100) overnight at 4°C. Then, a color-rendering reaction was conducted using the corresponding secondary antibodies. Subsequently, the stained sections were visualized and images were captured under a light microscope (Nikon Eclipse C1, Tokyo, Japan).

Immunofluorescence Analysis

Immunofluorescence (IF) staining of tissues involves several fundamental steps, including dewaxing and hydration. Subsequently, the corresponding primary antibodies were added and the samples were blocked with 5% BSA for 2 h before incubation. Then, the sections were incubated together with the fluorescent secondary antibodies at 4°C overnight. Following this, the sections were stained with DAPI for 5 min to visualize the nuclei and sealed, and the images were captured using a light microscope.

Western Blotting Analysis

A specified amount of primary astrocytes or mouse brain tissues were washed with precooled PBS, and subsequently treated with an appropriate protein lysate to extract proteins. After quantitative packaging, 100°C inactivated for 5–7 min. Following inactivation, the protein components were separated by 12% SDS-PAGE gel electrophoresis and transferred onto a PVDF membrane for 5% skim milk blocking for 2 h at room temperature. Subsequently, the membrane was incubated with primary antibodies overnight at 4°C, including SIRT3 (ab246522, Abcam), ATP5O (ab110276, Abcam), DRP1 (12,957-1-AP, Proteintech), MFN1 (13,798-1-AP, Proteintech), FIS1 (10,956-1-AP, Proteintech), MFN2 (12,186-1-AP, Proteintech), and GAPDH (ab8245, Abcam). After incubation with the corresponding secondary antibody based on the primary antibody source, the PVDF membrane was processed using an NcmECL High Kit (NCM Biotech, Suzhou, China).

Reverse Transcription-Quantitative PCR (qRT-PCR)

The mRNA expression levels in the samples were assessed through qRT-PCR experiments. Initially, total RNA was extracted using an RNA extraction kit (Vazyme, Nanjing, Jiangsu). The concentration of RNA was then determined using UV spectrophotometry. Following this, the RNA was reverse transcribed into cDNA using a cDNA synthesis supermix kit obtained from TransGen Biotech (Beijing). Finally, the $2^{\Delta\Delta CT}$ method was selected for the quantitative analysis of mRNA expression. The specific primer sequences are listed in Table S1.

Mitochondrial Membrane Potential (Δψm) Assay

The Mitochondrial membrane potential (ΔΨm) assay kit (Solarbio, Cat. M8650, Beijing, China) serves as an indicator of mitochondrial functional status. Detailed procedural instructions can be found in the kit's manual. Cells stained with the ΔΨm kit exhibited both orange and green fluorescence, and the comparison of their intensities provides insights into mitochondrial function. Specifically, an increase in orange fluorescence intensity signifies an elevation in mitochondrial membrane potential, whereas a decrease in orange fluorescence intensity indicates a reduction in membrane potential.

Detection of Reactive Oxygen Stress

The status of the cell was intimately linked to reactive oxygen stress (ROS) levels. To evaluate ROS, kits specifically designed for both cellular (CA1410, Solarbio) and mitochondrial (BB-46091, BestBio) ROS can be employed. Following the appropriate procedure, it allowed us to detect ROS levels in astrocytes in each group of mitochondria.

Transfection of SIRT3 shRNA

When the number of primary astrocytes grew to 60% of the surface of the culture dish, serum-free medium DMEM containing sh-SIRT3 or sh-NC was incubated for 12h. Among them, the primary astrocytes were cultured with sh-SIRT3 (ACAAGAACTGCTGGATCTTAT) and sh-NC (TTCTCCGAACGTGTCACGTTT) by GenePharma (Shanghai, China), while Lipofectamine 2000 (Invitrogen, Carlsbad, CA, USA) and shRNA were utilized in equal proportions.

Data Analysis

Data were analyzed using Graph Pad Prism 8.0 software with one-way ANOVA or Student's *t*-test between two groups. All results were presented as the average ± SEM derived from at least three independent experiments. In this study, number of $p<0.05$ indicated a statistically significant difference, while $p<0.01$ shown a highly significant difference.

Results

MET Rescues the HFD-Induced DACD in Mice

A mouse model of type 2 diabetes was constructed according to the same method.[23] Subsequently, to validate the success of the diabetes mellitus (DM) model, we tested the Insulin resistance, intraperitoneal glucose tolerance test (IPGTT) and fasting blood glucose (FBG). These results obtained demonstrated that insulin resistance, IPGTT were impaired, and FBG was significantly up-regulated in the model group, indicating the mouse model of type 2 diabetes was successfully established (Figure 1A–C). The results indicated that the elevated levels of total cholesterol (TC), triglyceride (TG), and low-density lipoprotein cholesterol (LDL-C), along with the decreased level of HDL-C observed in the model group, could be reversed following the administration of MET (Figure 1H). To evaluate the emotional and cognitive functional status of DM mice, the results showed that through FST and SPT experiments, mice in the model group had significantly increased swimming immobility time and significantly decreased sugar water preference than the normal group, which after MET treatment significantly reversed the changes (Figure 1D and E). Additionally, we further validated the effect of MET preconditioning on DM mice using MWM experiments, with representative swimming paths depicted in (Figure 1F). When compared to the control group, mice had increased total motor distance, decreased mean swimming speed, percentage of fourth quadrant entry and retention time ratio in the model group, however, were able to reverse the change after giving protection from MET (Figure 1G). Concurrently, an examination of mouse hippocampus pathology through Haematoxylin–eosin staining (H&E) revealed that the DACD group exhibited severe pyknotic nuclei and neuronal necrosis compared to the control group. However, these pathological changes were ameliorated by MET administration (Figure 1I). Taken together, the present findings demonstrate that MET is capable of significantly alleviating DACD symptoms in mice.

MET Suppresses Mitochondrial Dysfunction in DACD Mice

Maintaining the dynamic balance of mitochondria is crucial for DACD, prompting us to investigate the functional status of mitochondria in mice. Our observations in the DACD group revealed significant mitochondrial damage in the hippocampus. However, treatment with MET was found to significantly ameliorate these morphological alterations (Figure 2A). The functional state of mitochondria is closely linked to the mitochondrial fission fusion proteins. In the DACD group, DRP1 and FIS1 proteins were up-regulated, and MFN1 and MFN2 were down-regulated compared with the normal group. Importantly, MET treatment significantly modulated these protein levels, reversing the observed changes (Figure 2B and C). Sirtuins (SIRT) played a pivotal role in maintaining normal bodily functions, prompting us to assess the mRNA levels of SIRT1-7. The results showed that SIRT3 expression was down-regulated in the DACD group compared to the control group, and this change was reversible upon administering MET (Figure 2D). Western blotting experiments further confirmed that SIRT3 and ATP5O proteins were down-regulated in the DACD group compared with the control group. However, in the MET-treated group, the expression of SIRT3 and ATP5O proteins was up-regulated compared to the DACD group (Figure 2E and F). To further substantiate that MET improves DACD by modulating mitochondrial functional status, immunohistochemistry experiments were conducted, and the results were consistent with those obtained from the Western blot experiments (Figure 2G).

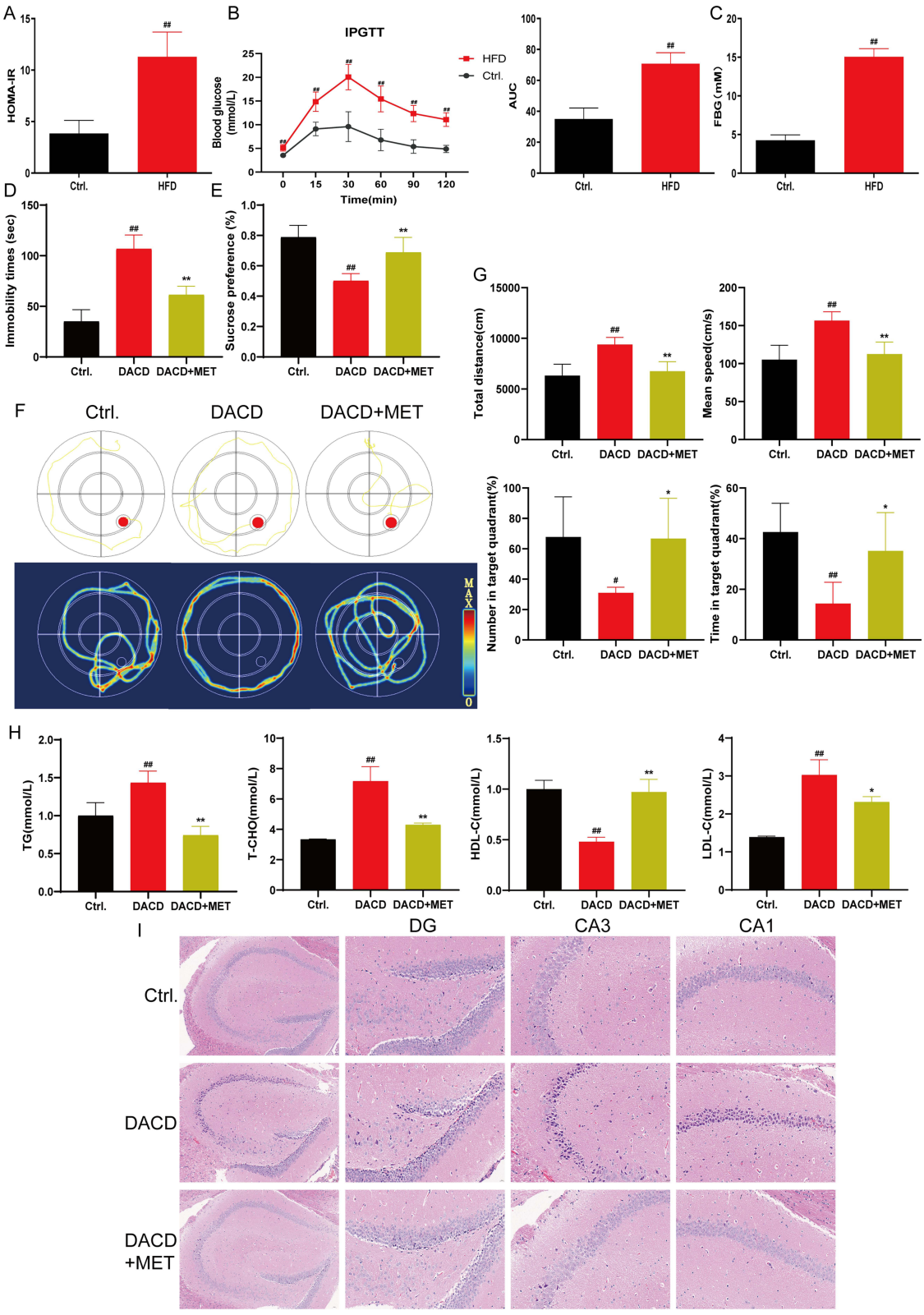

Figure 1 MET rescues the HFD-induced DACD in mice. (**A**) Insulin resistance indices in mice (n =6). (**B**) OGTT in different groups, AUC of blood glucose in mice (n =6). (**C**) Fasting blood glucose (FBG) in mice (n =6). (**D**) Mouse immobility time (n =6). (**E**) Sugar and water consumption rate (n =6). (**F**) Representative swimming path of the mice. (**G**) The statistics of the Total distance, Mean speed, Number in target quadrant and Time in target quadrant (n =6). (**H**) MET on the serum levels of TG, T-CHO, HDL-C and LDL-C (n =6). (**I**) Hippocampal tissue specimens were dyed with H&E (scale bar = 20 μm). $^{\#}p < 0.05$, $^{\#\#}p < 0.01$ versus the control group; $^{*}p < 0.05$, $^{**}p < 0.01$ versus the model group.

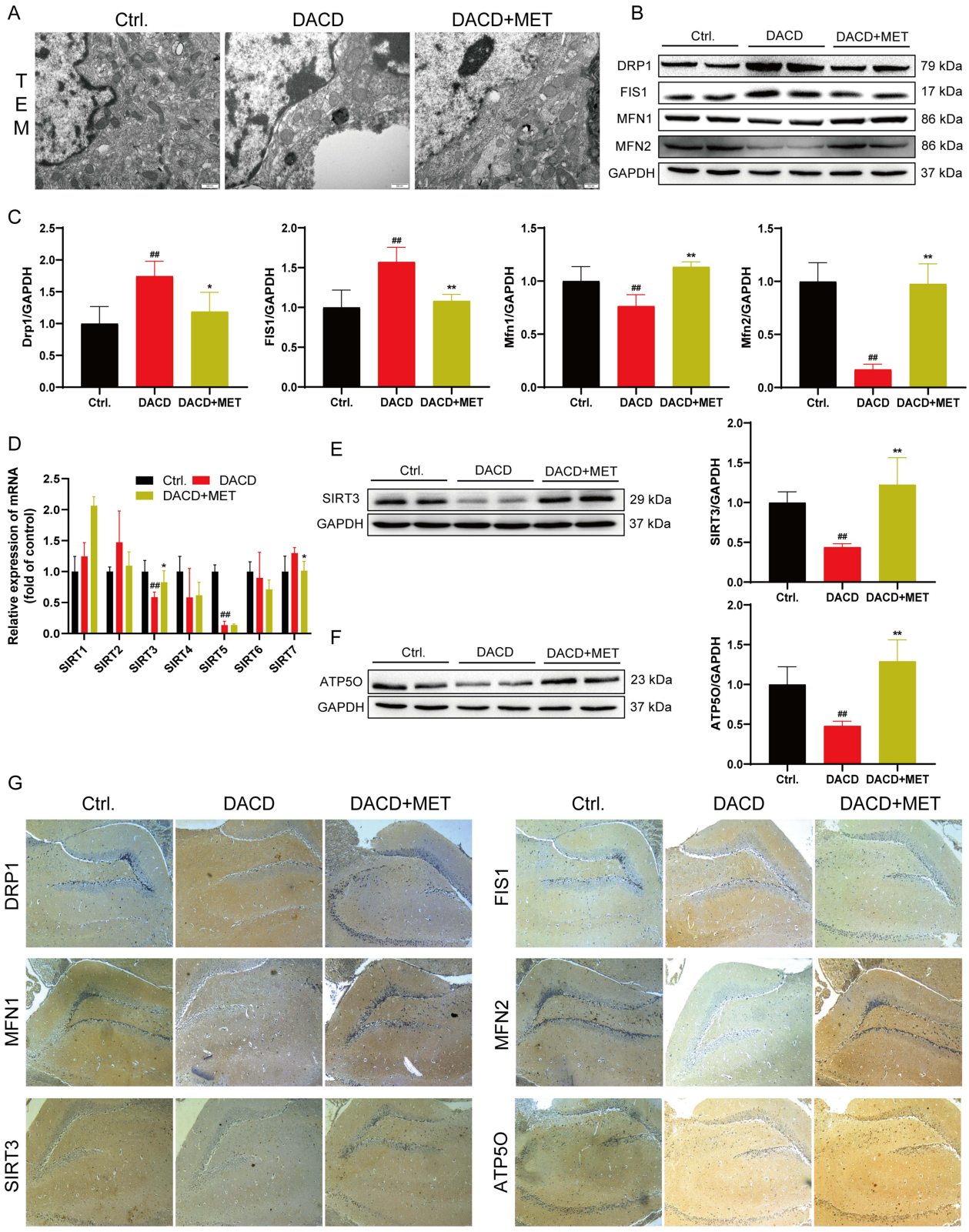

Figure 2 MET improves mitochondrial function in DACD mice. (**A**) Representative Transmission electron microscopy (TEM) images of mitochondria in the hippocampal tissue (scale bar = 500 nm). (**B** and **C**) Western blotting analysis of DRP1, FIS1, MFN1 and MFN2 protein levels in mouse hippocampal tissues (n = 4). (**D**) Detection of tissue SIRT1-SIRT7 mRNA levels in the hippocampus (n = 3). (**E** and **F**) SIRT3 and ATP5O protein levels were analysed by Western blotting (n = 4). (**G**) Representative images of DRP1, FIS1, MFN1 and MFN2 immunohistochemical dyeing (scale bar = 50 μm). $^{\#}p < 0.05$, $^{\#\#}p < 0.01$ versus the control group; $^{*}p < 0.05$, $^{**}p < 0.01$ versus the model group.

https://doi.org/10.2147/DMSO.S516173

MET Relies on SIRT3 to Alleviate Mitochondrial Dysfunction in HG/PA-Induced Primary AST

Given the diverse cellular composition of brain tissue, GFAP, Iba1, and Neun cell signature proteins were selected for immunofluorescence staining of brain sections. The results revealed that the immunofluorescence intensity of SIRT3 was decreased in the DACD group compared to the control group, and this decrease was inhibited in the MET-treated group. Notably, this change was consistent only in the GFAP-labeled tissue (Figure S1A). The purity of the isolated primary AST was specifically labeled with GFAP, and a purity above 90% was allowed for subsequent experimental studies (Figure S1B). To mimic the in vivo DACD model, high glucose/palmitic acid (HG/PA) induction in vitro was conducted. The optimal concentrations for HG/PA induction and MET protection were determined through MTT experiments, as illustrated in the figure (Figure S1C). Cellular oxidative stress levels, measured using the DCFH-DA fluorescent probe and Mito-ROS, indicated that both ROS and Mito-ROS were elevated in the DACD group compared to the control group. Notably, ROS levels were significantly reduced after pretreatment with MET (Figure 3A–D). The key proteins involved in maintaining mitochondrial function are DRP1, FIS1, MFN1, and MFN2. Western blot and qRT-PCR experiments revealed that DRP1 and FIS1 were up-regulated, while MFN1 and MFN2 were down-regulated in the DACD group compared to the control group. These changes were significant and reversible upon pretreatment with MET (Figure 3E, G and H). The membrane potential of mitochondria was examined by JC-1 fluorescence staining. Compared with the normal group, the DACD group showed decreased red fluorescence and increased green fluorescence, which indicated that the membrane potential of mitochondria was decreased, and then increased after administration of MET pre-protection (Figure 3F). Most importantly, the RNA levels and protein levels of SIRT3 also changed. Both RNA and protein levels were reduced in the DACD group compared with the control group, but MET was able to reverse this (Figure 3I). Meanwhile, the changes in RNA levels and protein levels of ATP5O were similar to those in the control group (Figure 3J).

Transfection of SIRT3 shRNA to Verify the Regulatory Mechanism of Mitochondrial Function by MET

To explore the effect of deleting sh-SIRT3 on the mitochondrial function of primary AST, the transfection efficiency of SIRT3 shRNA was examined by qRT-PCR, and we found that the knockdown of sh-SIRT3-925 was more effective (Figure 4A). The expression level of mitochondrial cleavage fusion protein was determined by Western blotting. The results showed that sh-SIRT3 suppressed the down-regulation of DRP1 and FIS1 protein levels and the up-regulation of MFN1 and MFN2 protein levels by MET (Figure 4B and C). Meanwhile, the protein level regulation of SIRT3 and ATP5O was identical (Figure 4D–F). Furthermore, a JC-1 (Figure 4G), Mito-ROS and ROS (Figure S1D and E) fluorescence staining was performed, and we found that sh-SIRT3 was able to significantly reduce the mitochondrial membrane potential, ROS and abrogate the protective effect of MET on mitochondrial function. In summary, knockdown of SIRT3 significantly inhibited the protective effect of MET on the mitochondrial function of primary AST.

MET Up-Regulates SIRT3 to Ameliorate Mitochondrial Dysfunction in the DACD

How elevated or decreased levels of SIRT3 expression affect the protective effects of MET was investigated. The SIRT3-specific agonist RES (1.5 μmol/L) and the inhibitor 3-TYP (50 nmol/L) were used to intervene in primary AST, to further explore whether SIRT3 is an important link in the protection of MET against the mitochondrial dysfunction in primary AST. The results of the Western blot experiments showed that RES significantly down-regulated the protein levels of DRP1 and FIS1, and also up-regulated the protein levels of MFN1 and MFN2 levels and also upregulated the protein levels of MFN1 and MFN2. However, 3-TYP significantly up-regulated the protein expression levels of DRP1 and FIS1, and down-regulated the protein expression levels of MFN1 and MFN2, eliminating the ameliorative effect of MET (Figure 5A). Meanwhile, changes in SIRT3 and ATP5O protein levels were similarly affected by the agonist RES and the inhibitor 3-TYP (Figure 5B and C). As mentioned above, SIRT3 is closely related to ATP5O, so Co-IP experiments were used to investigate the relationship between SIRT3 and ATP5O. The Co-IP results showed that SIRT3 interacted with ATP5O in primary AST, and MET was able to promote synergistic interactions between SIRT3 and ATP5O (Figure 5D).

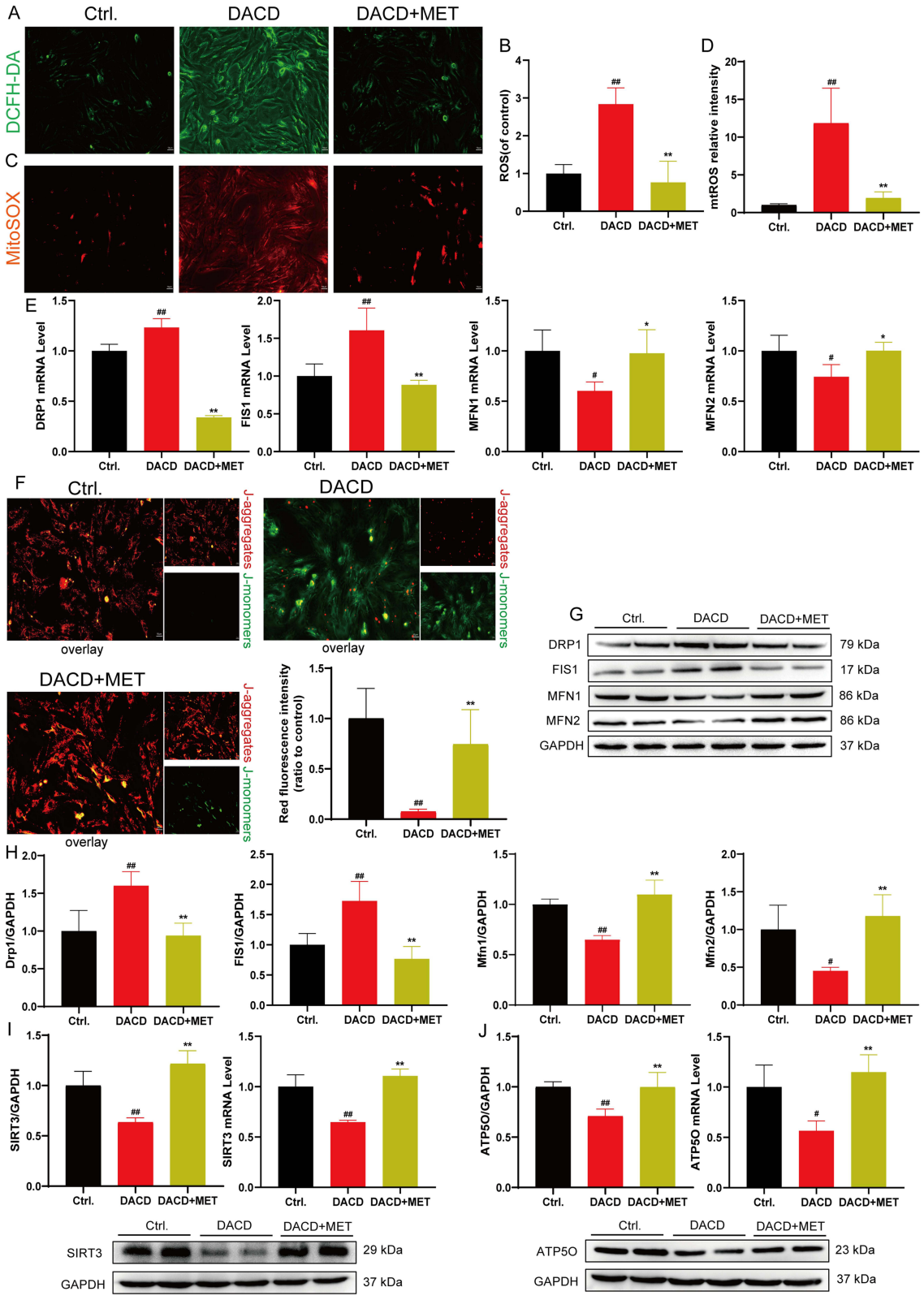

Figure 3 MET relies on SIRT3 to alleviate mitochondrial dysfunction in HG/PA-induced AST. (**A**) DCFH-DA fluorescence staining of AST (scale bar = 50 μm). (**B**) Quantitative analysis of the ROS (n = 5). (**C**) MitoSOX fluorescence staining of AST (scale bar = 50 μm). (**D**) Quantitative analysis of the MitoROS (n = 5). (**E**) Detection of DRP1, FIS1, MFN1 and MFN2 mRNA levels in the AST (n = 3). (**F**) Representative images of JC-1 dyeing and quantitative analysis (scale bar = 50 μm). (**G** and **H**) Western blotting analysis of DRP1, FIS1, MFN1 and MFN2 protein levels in AST (n = 4). (**I** and **J**) Analysis of SIRT3 and ATP5O protein and mRNA levels (n = 3). $^{\#}p < 0.05$, $^{\#\#}p < 0.01$ versus the control group; $^{*}p < 0.05$, $^{**}p < 0.01$ versus the model group.

https://doi.org/10.2147/DMSO.S516173

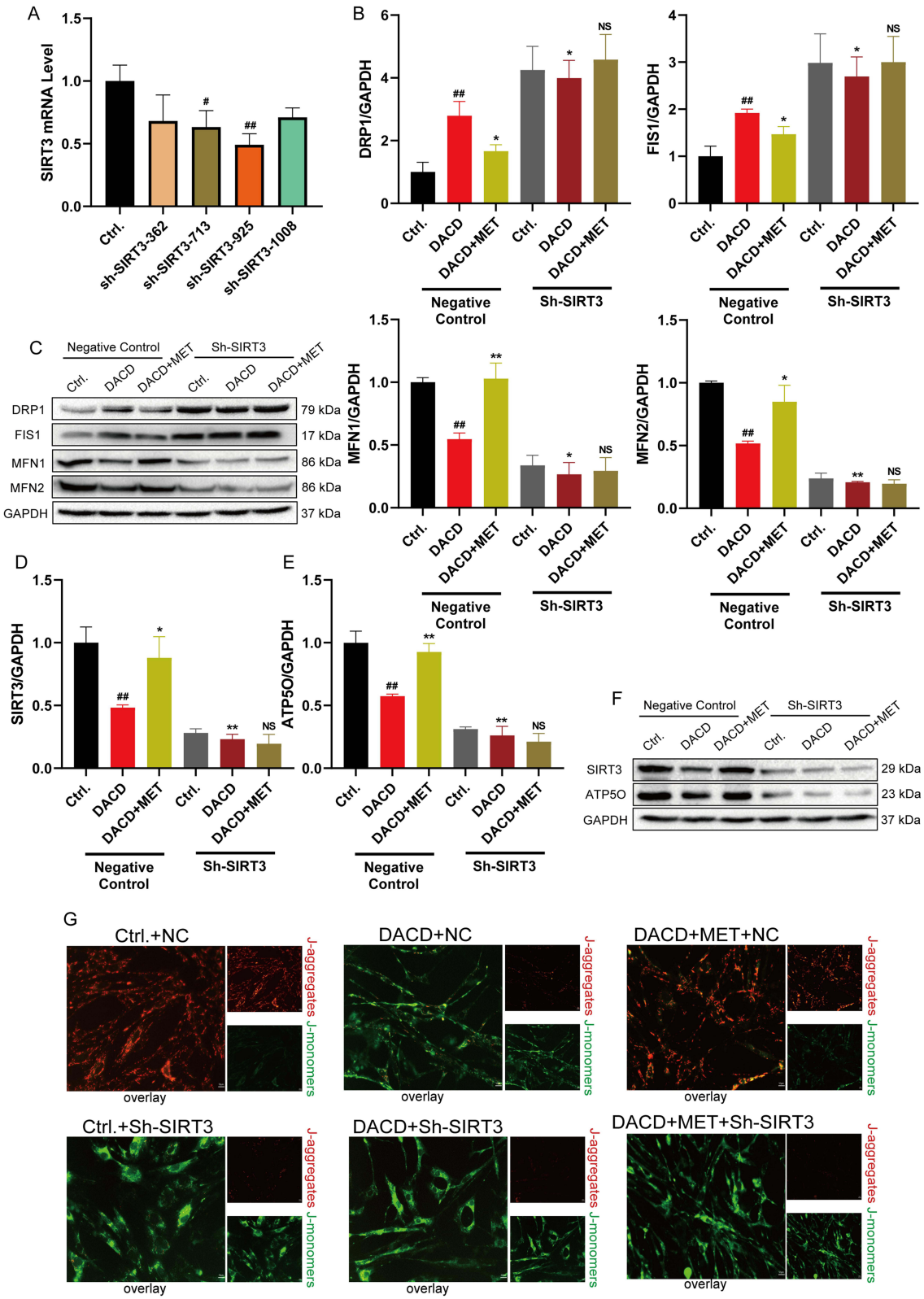

Figure 4 Transfection of SIRT3 shRNA to verify the regulatory mechanism of mitochondrial function by MET. (**A**) qRT-PCR for SIRT3 proteins in AST transfected with negative control and SIRT3 shRNA (n = 3). (**B** and **C**) Western blotting analysis of DRP1, FIS1, MFN1 and MFN2 protein levels after SIRT3 shRNA treatment in AST (n = 3). (**D**–**F**) Western blotting analysis of SIRT3 and ATP5O proteins in SIRT3 shRNA-transfected AST (n = 3). (**G**) Representative images of JC-1 dyeing (scale bar = 50 μm). $^{\#}p < 0.05$, $^{\#\#}p < 0.01$ versus the control group; $^{*}p < 0.05$, $^{**}p < 0.01$ versus the model group.

https://doi.org/10.2147/DMSO.S516173

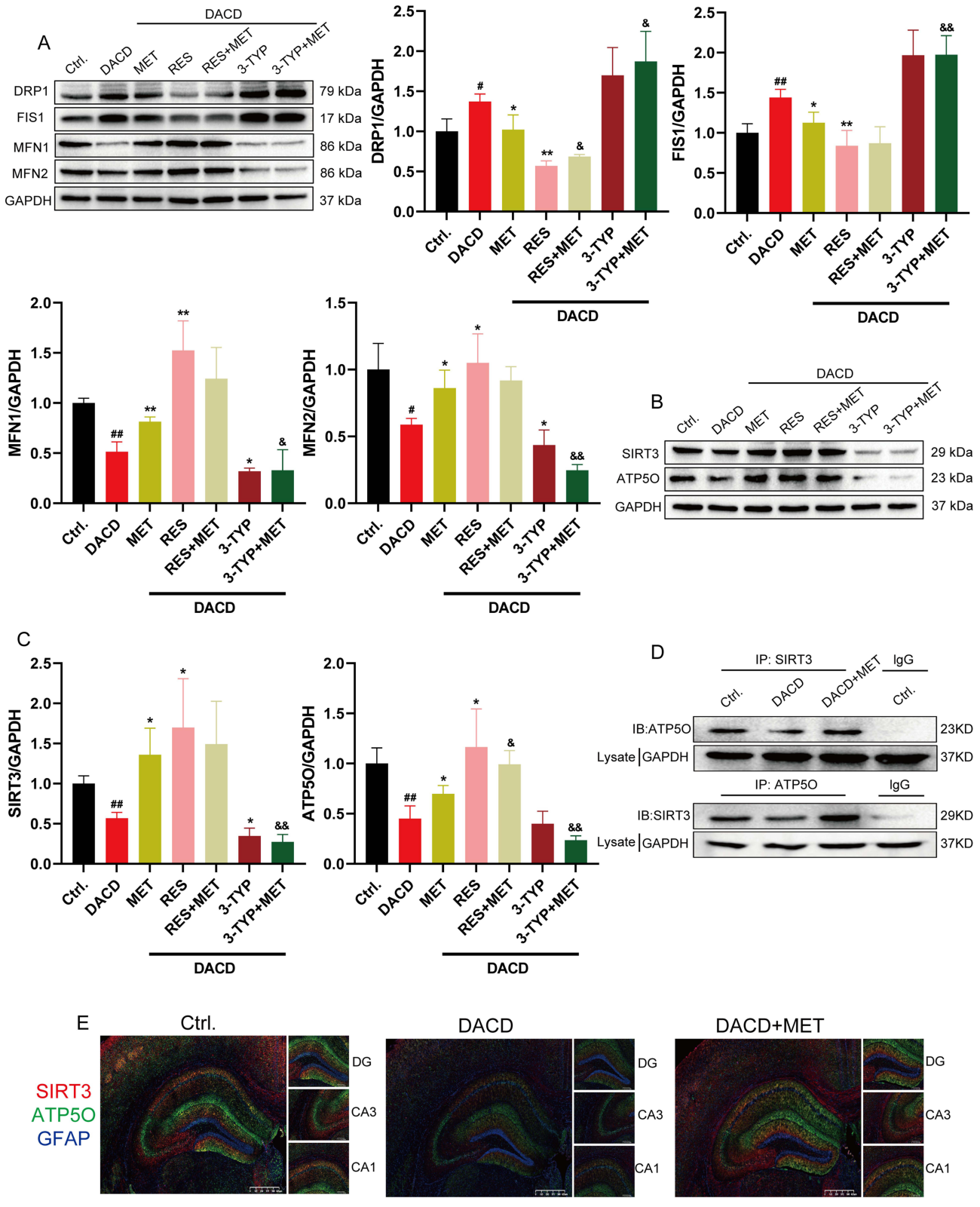

Figure 5 MET up-regulates SIRT3 to ameliorate mitochondrial dysfunction in the DACD. (**A**) The expression level of DRP1, FIS1, MFN1 and MFN2 proteins after RES or 3-TYP pre-treatment in NMVMs (n = 3). (**B** and **C**) Western blotting analysis of SIRT3 and ATP5O proteins (n = 3). (**D**) The interaction between SIRT3 and ATP5O in AST analysed by co-immunoprecipitation. (**E**) Immunofluorescence double staining of SIRT3 and ATP5O in the hippocampus (scale bar = 625 μm, scale bar = 200 μm). $^{\#}p < 0.05$, $^{\#\#}p < 0.01$ versus the control group; $^{*}p < 0.05$, $^{**}p < 0.01$ versus the model group; $^{\&}p < 0.05$, $^{\&\&}p < 0.01$ versus the CVB-D group.

https://doi.org/10.2147/DMSO.S516173

Moreover, reduced expression of SIRT3 and ATP5O in the DACD group was also observed in animal tissue sections. However, protection with MET increased the expression and interaction of SIRT3 and ATP5O (Figure 5E).

Discussion

Research indicates that diabetes-associated cognitive dysfunction (DACD) has emerged as the second leading cause of mortality among individuals with diabetes.[24] Despite this, the underlying pathological mechanisms of DACD remain inadequately understood, and there is an urgent need to investigate effective treatment strategies. Metformin (MET), a first-line therapy for type 2 diabetes, is extensively utilized in clinical settings due to its reliable hypoglycemic effects, favorable safety profile, and cost-effectiveness.[25] Notably, recent studies have revealed that MET's therapeutic benefits extend beyond glucose reduction, as it also contributes to ameliorating mitochondrial dysfunction and modulating oxidative stress levels.[26,27] This finding offers a significant insight into the potential application of MET in the context of DACD. Prior research has demonstrated that MET can mitigate hippocampal neuronal damage in diabetic mice by inhibiting excessive mitochondrial fission and reducing mitochondrial-derived oxidative stress, ultimately enhancing cognitive function.[13] In alignment with these previous studies, the current investigation also observed that MET markedly improved cognitive impairment and ameliorated hippocampal histopathological alterations in DACD mice.

Given the pivotal role of mitochondria in sustaining brain functional homeostasis, our investigation further concentrated on alterations in mitochondrial morphology. Transmission electron microscopy analysis revealed significant structural damage in the hippocampal mitochondria of the DACD group, whereas MET treatment effectively ameliorated this aberrant condition. These findings indicate that MET may mitigate the pathological progression of DACD by preserving mitochondrial structure and function. Nonetheless, the precise molecular targets of MET in modulating mitochondrial function remain unidentified. It is noteworthy that the Sirtuin family of proteins plays crucial roles in maintaining mitochondrial function. This family comprises seven members (Sirtuin 1–7), among which Sirtuin 3 (SIRT3) is specifically localized to the mitochondria.[15,28] As a NAD^+-dependent mitochondrial deacetylase, SIRT3 plays a crucial role in maintaining mitochondrial dynamics by regulating protein acetylation levels, thereby serving an indispensable function in mitigating mitochondrial dysfunction and oxidative stress damage.[29,30] Numerous studies have demonstrated that reduced SIRT3 activity results in the abnormal accumulation of acetylated mitochondrial proteins, which subsequently leads to impaired oxidative phosphorylation, excessive production of reactive oxygen species, and a decline in mitochondrial membrane potential.[31,32] In the present study, we observed that MET significantly upregulates SIRT3 expression, thereby enhancing mitochondrial functional status. Immunofluorescence co-localization analysis further indicated that MET predominantly increases SIRT3 expression in AST.

AST, as the most prevalent glial cells in the central nervous system, not only provide nutritional support to neurons but also play a crucial role in synapse formation and neural signal transmission.[33] In vitro experiments on primary AST demonstrated that the regulatory effects of MET on proteins related to mitochondrial fission and fusion were highly consistent with findings from animal studies. Further assessment of mitochondrial membrane potential confirmed that MET effectively mitigated mitochondrial damage associated with DACD. To elucidate the mediating role of SIRT3, we employed Sh-SIRT3 to suppress SIRT3 expression in AST, revealing that SIRT3 knockdown completely abrogated the therapeutic effects of MET. Moreover, intervention experiments using a SIRT3 agonist (resveratrol) and inhibitor (3-TYP) substantiated that MET enhances ATP5O expression through the activation of the SIRT3 signaling pathway, thereby ameliorating mitochondrial dysfunction.

This study establishes a novel experimental foundation for the clinical application of MET and identifies a potential target for the development of therapeutic strategies aimed at addressing DACD. Nevertheless, this study has several limitations that need to be considered. First, we did not include female mice in the research. Additionally, it is important to note that while the data indicate an interaction between SIRT3 and ATP5O, the precise molecular mechanism through which SIRT3 regulates ATP5O remains to be elucidated in greater detail. In conclusion, the current investigation demonstrates that MET may ameliorate mitochondrial dysfunction associated with DACD by activating the SIRT3 signaling pathway, thereby offering a new mechanistic insight into its neuroprotective effects.

Conclusions

In summary, our findings indicate that MET activation of the SIRT3 signaling pathway and the upregulation of ATP5O, which mitigates mitochondrial damage and dysfunction in AST, and plays a protective role in the cognitive impairment of DACD. This study elucidates the molecular mechanisms underlying the beneficial effects of MET on DACD and offers a reference point for the development of therapeutic strategies for DACD-related conditions.

Abbreviations

DACD, Diabetes-associated cognitive dysfunction; HFD, high-fat diet; MET, metformin; STZ, streptozotocin; AST, Astrocytes; RES, resveratrol; ROS, reactive oxygen species; ATP5O, ATP synthase subunit O; TEM, transmission electron microscope; IF, Immunofluorescence; MMP, mitochondrial membrane potential; GAPDH, housekeeping protein.

Data Sharing Statement

The data that support the findings of this study are available from the corresponding author upon reasonable request.

Acknowledgments

This project was approved by the National Natural Science Foundation of China [No. 82060729, U1812403-4-4], the Guizhou Provincial Science and Technology projects ([2020]1Z069), the Guizhou Provincial Scientific and Technologic Innovation Base ([2023]003), and the High level Innovation Talents (No. GCC [2023]048).

Disclosure

The authors declare that they have no conflict of interest.

References

1. Liu J, Liu L, Han Y, et al. The molecular mechanism underlying mitophagy-mediated hippocampal neuron apoptosis in diabetes-related depression. *J Cell Mol Med*. 2021;25(15):7342–7353. doi:10.1111/jcmm.16763
2. Gao Y, Xiao Y, Miao R, et al. The prevalence of mild cognitive impairment with type 2 diabetes mellitus among elderly people in China: a cross-sectional study. *Arch Gerontol Geriatr*. 2016;62:138–142. doi:10.1016/j.archger.2015.09.003
3. Jiang Z, Liu B, Lu T, et al. SGK1 drives hippocampal demyelination and diabetes-associated cognitive dysfunction in mice. *Nat Commun*. 2025;16(1):1709. doi:10.1038/s41467-025-56854-2
4. Jiang T, Li Y, He S, et al. Reprogramming astrocytic NDRG2/NF-kappaB/C3 signaling restores the diabetes-associated cognitive dysfunction. *EBioMedicine*. 2023;93:104653. doi:10.1016/j.ebiom.2023.104653
5. Habib N, Mccabe C, Medina S, et al. Disease-associated astrocytes in Alzheimer's disease and aging. *Nat Neurosci*. 2020;23(6):701–706. doi:10.1038/s41593-020-0624-8
6. Chalmers N, Masouti E, Beckervordersandforth R. Astrocytes in the adult dentate gyrus-balance between adult and developmental tasks. *Mol Psychiatry*. 2024;29(4):982–991. doi:10.1038/s41380-023-02386-4
7. Nation DA, Sweeney MD, Montagne A, et al. Blood-brain barrier breakdown is an early biomarker of human cognitive dysfunction. *Nat Med*. 2019;25(2):270–276. doi:10.1038/s41591-018-0297-y
8. Zheng J, Xie Y, Ren L, et al. GLP-1 improves the supportive ability of astrocytes to neurons by promoting aerobic glycolysis in Alzheimer's disease. *Mol Metab*. 2021;47:101180. doi:10.1016/j.molmet.2021.101180
9. Sun C, Liu X, Wang B, et al. Endocytosis-mediated mitochondrial transplantation: transferring normal human astrocytic mitochondria into glioma cells rescues aerobic respiration and enhances radiosensitivity. *Theranostics*. 2019;9(12):3595–3607. doi:10.7150/thno.33100
10. Cheng X, Vinokurov AY, Zherebtsov EA, et al. Variability of mitochondrial energy balance across brain regions. *J Neurochem*. 2021;157(4):1234–1243. doi:10.1111/jnc.15239
11. Proulx JM, Park I, Borgmann K. HIV-1 and methamphetamine co-treatment in primary human astrocytes: tAARgeting ER/UPR dysfunction. *NeuroImmune Pharm Ther*. 2024;3(2):139–154. doi:10.1515/nipt-2023-0020
12. Maneechote C, Chunchai T, Apaijai N, Chattipakorn N, Chattipakorn SC. Pharmacological targeting of mitochondrial fission and fusion alleviates cognitive impairment and brain pathologies in pre-diabetic rats. *Mol Neurobiol*. 2022;59(6):3690–3702. doi:10.1007/s12035-022-02813-7
13. Hu Y, Zhou Y, Yang Y, et al. Metformin protects against diabetes-induced cognitive dysfunction by inhibiting mitochondrial fission protein DRP1. *Front Pharmacol*. 2022;13:832707. doi:10.3389/fphar.2022.832707
14. Li P, Newhardt MF, Matsuzaki S, et al. The loss of cardiac SIRT3 decreases metabolic flexibility and proteostasis in an age-dependent manner. *Geroscience*. 2023;45(2):983–999. doi:10.1007/s11357-022-00695-0
15. Chang Y, Wang C, Zhu J, et al. SIRT3 ameliorates diabetes-associated cognitive dysfunction via regulating mitochondria-associated ER membranes. *J Transl Med*. 2023;21(1):494. doi:10.1186/s12967-023-04246-9
16. Gimenez-Escamilla I, Benedicto C, Perez-Carrillo L, et al. Alterations in mitochondrial oxidative phosphorylation system: relationship of complex V and cardiac dysfunction in human heart failure. *Antioxidants*. 2024;13(3):285. doi:10.3390/antiox13030285

17. Alavian KN, Beutner G, Lazrove E, et al. An uncoupling channel within the c-subunit ring of the F1FO ATP synthase is the mitochondrial permeability transition pore. *Proc Natl Acad Sci U S A*. 2014;111(29):10580–10585. doi:10.1073/pnas.1401591111
18. Song Y, Wang J, Sun J, et al. Screening of potential biomarkers for gastric cancer with diagnostic value using label-free global proteome analysis. *Genomics Proteomics Bioinf*. 2020;18(6):679–695. doi:10.1016/j.gpb.2020.06.012
19. Yang W, Zhang K, Zhang Z, et al. Claudin-10 overexpression suppresses human clear cell renal cell carcinoma growth and metastasis by regulating ATP5O and causing mitochondrial dysfunction. *Int J Biol Sci*. 2022;18(6):2329–2344. doi:10.7150/ijbs.70105
20. ElSayed NA, Aleppo G, Bannuru RR. 9. pharmacologic approaches to glycemic treatment: standards of care in diabetes—2024. *Diabetes Care*. 2024;47(Suppl 1):S158–S178. doi:10.2337/dc24-S009
21. Lamoia TE, Shulman GI. Cellular and molecular mechanisms of metformin action. *Endocr Rev*. 2021;42(1):77–96. doi:10.1210/endrev/bnaa023
22. Xu G, Li T, Huang Y. The effects of intraoperative hypothermia on postoperative cognitive function in the rat hippocampus and its possible mechanisms. *Brain Sci*. 2022;12(1):96. doi:10.3390/brainsci12010096
23. Liao J, Fu L, Tai S, et al. Essential oil from Fructus Alpiniae zerumbet ameliorates vascular endothelial cell senescence in diabetes by regulating PPAR-gamma signalling: a 4D label-free quantitative proteomics and network pharmacology study. *J Ethnopharmacol*. 2024;321:117550. doi:10.1016/j.jep.2023.117550
24. Al-Akl NS, Khalifa O, Ponirakis G, et al. Untargeted metabolomic profiling reveals differentially expressed serum metabolites and pathways in type 2 diabetes patients with and without cognitive decline: a Cross-Sectional study. *Int J Mol Sci*. 2024;25(4):2247. doi:10.3390/ijms25042247
25. Cuatrecasas G, De Cabo F, Coves MJ, et al. Dapagliflozin added to metformin reduces perirenal fat layer in type 2 diabetic patients with obesity. *Sci Rep*. 2024;14(1):10832. doi:10.1038/s41598-024-61590-6
26. Ay M, Charli A, Langley M, et al. Mito-metformin protects against mitochondrial dysfunction and dopaminergic neuronal degeneration by activating upstream PKD1 signaling in cell culture and MitoPark animal models of Parkinson's disease. *Front Neurosci*. 2024;18:1356703. doi:10.3389/fnins.2024.1356703
27. Fernandez-Valero A, Pena-Montero N, Lima-Rubio F, et al. Changes in oxidative stress and intestinal permeability during pregnancy in women with gestational diabetes mellitus treated with metformin or insulin and healthy controls: a randomized controlled trial. *Antioxidants*. 2023;12(11):1981. doi:10.3390/antiox12111981
28. Molaei A, Molaei E, Hayes AW, Karimi G. Mas receptor: a potential strategy in the management of ischemic cardiovascular diseases. *Cell Cycle*. 2023;22(13):1654–1674. doi:10.1080/15384101.2023.2228089
29. Peng F, Liao M, Jin W, et al. 2-APQC, a small-molecule activator of Sirtuin-3 (SIRT3), alleviates myocardial hypertrophy and fibrosis by regulating mitochondrial homeostasis. *Signal Transduct Target Ther*. 2024;9(1):133. doi:10.1038/s41392-024-01816-1
30. Ren J, Chen X, Zhou L, et al. Protective role of sirtuin3 (SIRT3) in oxidative stress mediated by hepatitis b virus x protein expression. *PLoS One*. 2016;11(3):e150961. doi:10.1371/journal.pone.0150961
31. Chen C, Mcdonald D, Blain A, et al. Parkinson's disease neurons exhibit alterations in mitochondrial quality control proteins. *NPJ Parkinsons Dis*. 2023;9(1):120. doi:10.1038/s41531-023-00564-3
32. Huang B, Ding J, Guo H, et al. SIRT3 regulates the ROS-FPR1/HIF-1alpha axis under hypoxic conditions to influence lung cancer progression. *Cell Biochem Biophys*. 2023;81(4):813–821. doi:10.1007/s12013-023-01180-x
33. Bellaver B, Povala G, Ferreira PCL, et al. Astrocyte reactivity influences amyloid-beta effects on tau pathology in preclinical Alzheimer's disease. *Nat Med*. 2023;29(7):1775–1781. doi:10.1038/s41591-023-02380-x